Title

Correction to Selective Carbon Dioxide Adsorption by Two Robust Microporous Coordination Polymers

Journal

Inorganic Chemistry, 56(1)

ISSN

0020-1669

Authors

An, Litao

Wang, Hao

Teat, Simon J

et al.

Publication Date

2017-01-03

DOI

10.1021/acs.inorgchem.6b02919

Peer reviewed

Selective Carbon Dioxide Adsorption by Two Robust Microporous Coordination Polymers

Litao An,[†‡] Hao Wang,[‡] Simon J. Teat,[#] Feng Xu,[‡] Xin-Long Wang,[‡] Fangming Wang,[‡] and Jing Li[‡,*]

[†]Jiangsu Key Laboratory for Chemistry of Low-Dimensional Materials, College of Chemistry and Chemical Engineering, Huaiyin Normal University, Huaian 223300, China

[‡]Department of Chemistry and Chemical Biology, Rutgers University, 610 Taylor Road, Piscataway, New Jersey 08854, United States

[#]Advanced Light Source, Lawrence Berkeley National Laboratory, 1 Cyclotron Road, Berkeley, California 94720, United States

ABSTRACT

In the present work we report the design, synthesis, crystal structure determination, and adsorption properties of two new cadmium-based porous coordination polymers, $[Cd(pda)_{0.5}(spiro\text{-}4\text{-}py)_{0.5}(HCOO)]\bullet 2H_2O\bullet DMF$ (compound **1**, pda = p-phenylenediacetate, spiro-4-py = (2,2',7,7'-tetra(pyridin-4-yl)-9,9'-spirobi[fluorene], DMF = N,N'-dimethylformamide) and $[Cd_2(pda)(spiro\text{-}4\text{-}py)(CH_3COO)_2]\bullet DMA$ (compound **2**, DMA = N,N'-dimethylacetamide) with similar structures. The coordination between cadmium and two organic linkers, pda and spiro-4-py, has yielded two-dimensional frameworks with rhombic openings. Stacking of these two-dimensional networks does not block the openings but rather results in permanent porosity with one-dimensional channels in the final structures. The permanent porosity of these compounds is confirmed by gas adsorption measurements. Compounds **1** and **2** have BET (Brunauer-Emmett-Teller) surface areas of 687 and 584 m^2/g, respectively. Both compounds show favorable adsorption towards carbon dioxide over other light gases such as nitrogen, oxygen, and carbon monoxide. IAST (Ideal adsorbed solution theory) is employed to predict the adsorption selectivity of binary gas mixtures. Though compounds **1** and **2** possess similar structures, differences are observed in their gas adsorption behaviors, which can be attributed to their different terminal ligands of formate and acetate, respectively. Strikingly, both compounds show exceptionally high stability in aqueous media with a wide pH range, a characteristic that is highly desirable for gas separation-related applications. The robustness of these structures suggests that the use of hydrophobic spiro based multipyridine ligands can lead to water stable frameworks built on late-transition metals that are otherwise sensitive to moisture.

INTRODUCTION

Porous coordination polymers (PCPs) or metal-organic frameworks (MOFs) have emerged as a new class of crystalline, porous, multifunctional materials.[1,2] PCPs/MOFs are currently being studied for various applications, among which gas adsorption and separation have been well-investigated and have proven most fruitful.[3-11] PCPs/MOFs hold promise as a new generation of sorbent materials for industrially relevant gas storage and separation, due not only to their inherently high porosity, but also, more importantly, to their structure diversity and tunability. While the use of a variety of metal ions/clusters contributes to the structure diversity of PCPs/MOFs, their versatility arises largely from the diversity of organic ligands incorporated into the structures. Compared to traditional porous materials such as zeolites, PCPs/MOFs can be designed and tuned in terms of their structure, porosity, pore size, and functionality by judicious design/selection of organic ligands.[12,13] This means that targeted applications can be taken into account from the beginning of materials design and preparation. For example, isoreticular expansion has been commonly employed in the construction of PCPs/MOFs.[14-16] Pore volume and pore size are systematically tuned by controlling the length of the organic ligands, while their overall connectivity, which is determined by the geometry and main functionality of the ligands, is retained. By adding different functional groups to the organic ligands, one can also tune the functionality of PCPs without altering their overall structure.[17,18] In these ways, PCPs/MOFs with predictable structures and desirable properties can be designed and synthesized. The demand for creating new PCP/MOF materials has, in turn, spurred the development of organic synthesis. Over the past decade, a huge family of organic ligands has been designed, synthesized, and successfully incorporated into PCPs/MOFs, an advance that has contributed largely to the diversity of their structure, porosity, and functionality.[19,20]

Carbon dioxide capture has acquired global focus as a way of alleviating the greenhouse effect, which largely arises from worldwide energy consumption. Benefitting from their tunable porosity and functionality, PCPs/MOFs hold promises to address this challenging issue. Over the past two decades, numerous compounds in this material family have been designed and investigated for selective carbon dioxide capture from flue gas; significant progress has been reported.[4,21-27] However, developing new structures with good moisture/water stability and excellent carbon dioxide adsorption selectivity remains to be of high demand. Herein, we report the synthesis of a new organic ligand, spiro-4-py, and its incorporation into two novel porous coordination polymers. These polymers feature two-dimensional layered structures with permanent porosity and high resistance towards aqueous solutions. Both materials show selective carbon dioxide adsorption over other light gases.

EXPERIMETAL SECTION

Reagents and Methods. All starting materials used in this work were purchased from commercial providers (Fisher Scientific or VWR) and used as received without further purification. Nuclear magnetic resonance (NMR) data were collected on a 300 MHz Oxford NMR. Single-crystal synchrotron X-ray diffraction data were collected on a D8 goniostat equipped with a Bruker APEXII CCD detector at Beamline 11.3.1 at the Advanced Light Source (ALS) at Lawrence Berkeley National Laboratory, using synchrotron radiation tuned to λ= 0.7749 Å. The structure was solved by direct methods and refined by full-matrix least-squares on F^2 using the Bruker SHELXTL package. Powder X-ray diffraction (PXRD) analyses were carried out on a Rigaku Ultima-IV diffractomter using Cu Kα radiation (λ= 1.5406 Å). The data were collected at room temperature in a 2θ range of 3-50° with a scan speed of 1°/min. The operating

power was 40kV/40mA. Thermogravimetric analyses (TGA) of samples were performed using the TA Instrument Q5000 with nitrogen flow and sample purge rate at 10 cc/min and 25 cc/min, respectively. For each measurement, about 3 mg of sample was loaded onto a platinum sample pan and heated from room temperature to 600 °C at a rate of 10 °C/min under nitrogen flow. Gas adsorption measurements were performed on a 3Flex volumetric adsorption analyzer (Micromeritics Instrument Corporation) equipped with a Smart VacPrep outgassing unit. Ultra-high purity (99.999%) nitrogen and carbon dioxide were used. Liquid nitrogen was used as coolant for measurements at 77 K, and a digital heated circulating bath was used for temperature control around room temperature with water/ethylene glycol mixture as coolant. Around 150 mg of as synthesized MOF sample was activated at 150 °C under vacuum overnight prior to gas adsorption measurements. Between each measurement the sample was reactivated for 2 hours under the same conditions.

Ligand synthesis. The organic ligand spiro-4-py was synthesized as following.

A mixture of K_3PO_4 (8.06 g, 38.0 mmol), water (20 mL), 2,2',7,7'-tetrabromo-9,9'-spirobi[fluorene] (2 g, 3.16 mmol), 4-pyridineboronic acid (2.33 g, 19.0 mmol), and N,N-dimethylformamide (DMF, 100 mL) was added to a 250 mL 3-necked flask. The reaction mixture was deoxygenated by bubbling argon through the solution for 20 min. Palladium acetate (0.25 g, 1.11 mmol) and tricyclohexylphosphine (0.44 g, 1.58 mmol) were then added, and the

reaction mixture was heated to reflux for 4 days under argon atmosphere. After cooling to room temperature, the organic solvent was evaporated to dryness under vacuum. Water (100 mL) was added to the residue, and the mixture was extracted with chloroform (50 mL × 3). The combined organic phase was washed with water and brine and dried over anhydrous $MgSO_4$. The pure product (1.29 g, 65% yield) was obtained by column chromatography (20% methanol in ethyl acetate). ^{1}H NMR ($CDCl_3$, 300 MHz): 8.47-8.45 (m, 8H), 8.05 (d, *J* = 9Hz, 4H), 7.71-7.75 (m, 4H), 7.31-7.33 (m, 8H), 7.05 (d, *J* = 3Hz, 4H). ^{13}C NMR ($CDCl_3$, 75 MHz): 150.1, 149.5, 147.6, 141.9, 138.5, 127.5, 122.5, 121.5, 121.4, 66.1. MS (ESI) $C_{45}H_{29}N_4$ calculated 625.2, found 625.6 (M^+).

Synthesis of compound 1. A mixture of $Cd(NO_3)_2 \cdot 4H_2O$ (0.015 g, 0.049 mmol), spiro-4-py (0.015 g, 0.024 mmol), 1,4-PDA (*p*-phenylenediacetic acid, 0.009 g, 0.046 mmol), HBF_4 (2 drops), H_2O (2 mL), and DMF (8 mL) was added to a 20 mL scintillation vial and heated at 80 °C for 6 days. After being cooled to room temperature, slightly yellow block-shaped crystals were obtained by filtration, washed with DMF, and dried in air. Elemental analyses calcd (%) for $C_{28.5}H_{23}CdN_2O_6$ (601.92): C, 56.87; H, 3.85; N, 4.65; Found C, 56.85; H, 3.52; N, 4.80. IR (KBr pellet, cm^{-1}): 3414 (m), 2937 (w), 1606 (s), 1553 (m), 1468 (w), 1395 (s), 1262 (w), 1226 (w), 1069 (w), 1021 (w), 820 (m), 720 (w), 626 (w).

Synthesis of compound 2. A mixture of $Cd(NO_3)_2 \cdot 4H_2O$ (0.015 g, 0.049 mmol), spiro-4-py (0.015 g, 0.024 mmol), 1,4-PDA (0.010 g, 0.051 mmol), HBF_4 (2 drops), H_2O (1 mL), and DMA (4 mL) was added to a 20 mL scintillation vial and heated at 90 °C for 4 days. After being cooled to room temperature, slightly yellow block crystals were obtained by filtration, washed with DMF, and dried in air. Elemental analyses calcd (%) for $C_{59}H_{42}Cd_2N_4O_8$ (1159.83): C, 61.09; H,

3.65; N, 4.83; Found C, 56.93; H, 3.66; N, 4.82. IR (KBr pellet, cm^{-1}): 3424 (s), 2928 (w), 1672 (m), 1607 (s), 1560 (s), 1466 (w), 1392 (s), 1256 (w), 1226 (w), 1069 (w), 1020 (w), 817 (m), 720 (w), 626 (w).

Table 1. Crystal Data for compounds **1** and **2**

	Compound **1**	Compound **2**
Empirical formula	$C_{28.5}H_{23}CdN_2O_6$	$C_{59}H_{42}Cd_2N_4O_8$
Crystal system	Monoclinic	Monoclinic
Space group	P2/*c*	P2/*c*
a [Å]	10.5785(5)	10.4985(4)
b [Å]	14.4939(6)	14.5262(5)
c [Å]	20.5000(9)	20.6360(8)
α [°]	90	90
β [°]	97.355(2)	97.611(2)
γ [°]	90	90
Volume [$Å^3$]	3117.2(7)	3119.3(3)
Z	4	2
Density [g cm^{-3}]	1.220	1.282
R1 for $F_0^2 > 2\sigma(F_0^2)$	0.0504	0.0466
wR2	0.0757	0.1170
CCDC No.	1502463	1502464

Isosteric heat of adsorption. Carbon dioxide adsorption isotherms at three different temperatures (278, 288 and 298 K) were first fitted with the following virial equation:[28,29]

$$\ln(p) = \ln(v) + (1/T)\sum_{i=0}^{m} a_i v^i + \sum_{j=0}^{n} b_j v^j$$

Where v, p, and T are adsorbed amount, pressure, and temperature, respectively. The fitting parameter a_i is used in direct evaluation of Q_{st}

$$Q_{st} = -R\sum_{i=0}^{m} a_i v^i$$

Where R is the universal gas constant.

IAST selectivity. Adsorption selectivity of j over i is given by

$$S_{ji} = \left(\frac{x_j}{y_j}\right)\left(\frac{y_i}{x_i}\right)$$

Where x_m and y_m are the mole fraction of component m (m= i or j) in the adsorbed phase and bulk phase, respectively. The single component adsorption isotherms have been fitted to the following dual site Langmuir-Freundlich (DSLF) model to enable the application of the IAST calculation.[30-33]

$$N = N_1^{\max} \cdot \frac{b_1 p^{1/n_1}}{1 + b_1 p^{1/n_1}} + N_2^{\max} \cdot \frac{b_2 p^{1/n_2}}{1 + b_2 p^{1/n_2}}$$

Here, p is the pressure of the bulk gas at equilibrium with the adsorbed phase (kPa), N is the adsorbed amount per mass of adsorbent (mol/kg), $N_1^{\max}$ and $N_2^{\max}$ are the saturation capacities of sites 1 and 2 (mol/kg), b_1 and b_2 are the affinity coefficients of sites 1 and 2 (1/kPa), and n_1 and n_2 represent the deviations from an ideal homogeneous surface.

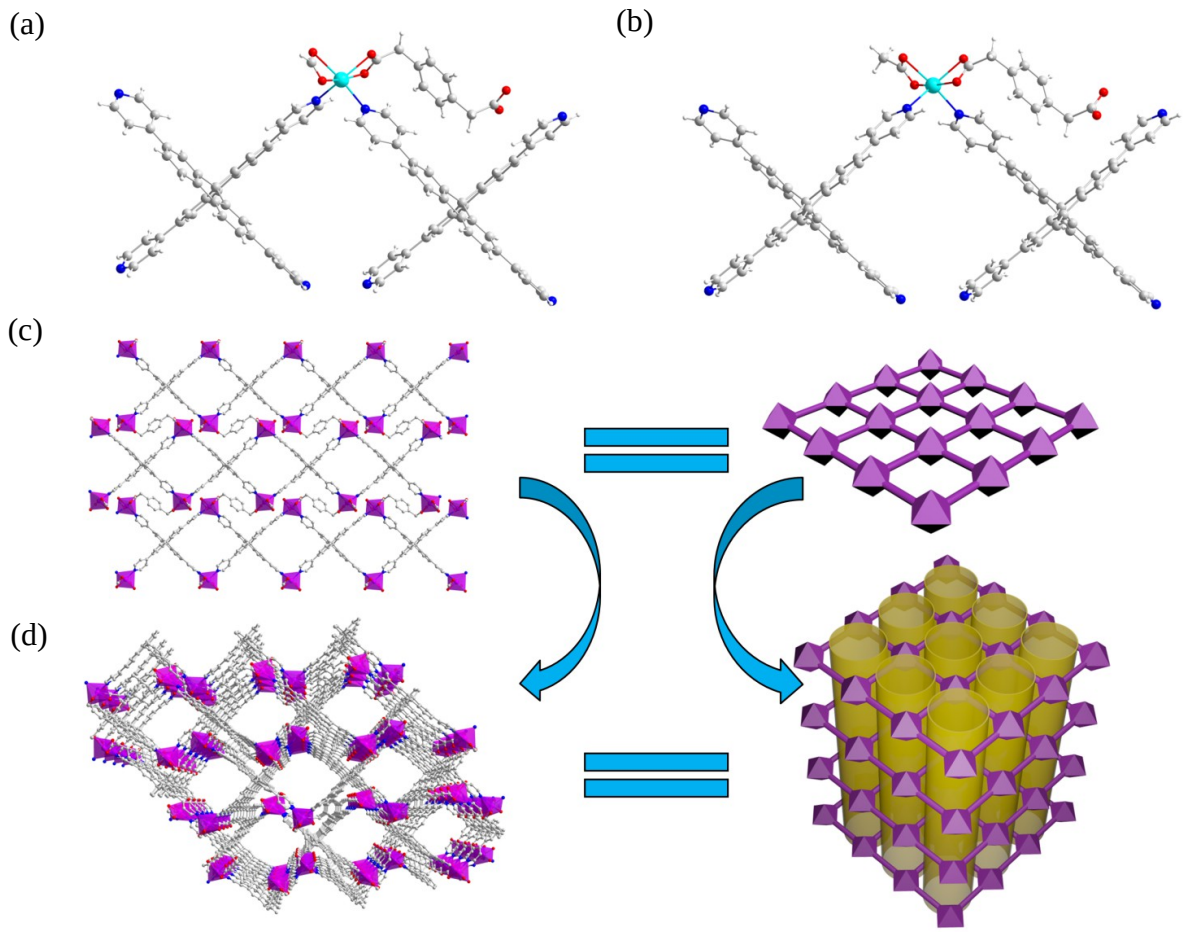

Figure 1. Structure illustration of compounds **1** and **2**. Coordination of cadmium in compounds **1** (a) and **2** (b). (c) Two-dimensional rhomboid grid and (d) view of one-dimensional channel in the two structures. Color scheme: Cd: cyan, O: red, N: blue, C: grey, H: white. Purple polyhedra represent Cd centers.

RESULTS AND DISCUSSION

Synthesis and crystal structure. Compounds **1** and **2** were synthesized solvothermally by mixing $Cd(NO_3)_2 \cdot 4H_2O$, spiro-4-py, and H_2pda in a mixed solvent (DMF for **1** and DMA for **2**, H_2O, and HBF_4) at 80 °C and 90 °C, respectively. Single crystal X-ray diffraction analysis shows that compounds **1** and **2** are isostructures but differ in terminal ligand on the metal center. The

terminal-coordinated formate and acetate in compounds **1** and **2** should result from the acid-catalyzed decomposition of DMF and DMA, respectively, as commonly seen in MOF synthesis.[34,35] Both compounds crystallize in the monoclinic space group P2/*c* (see Table 1 and Supporting Information for detail). There is only one crystallographically independent cadmium center in the structure. It has a distorted octahedral geometry and is six-coordinated to one pda through oxygen, two spiro-4-py through nitrogen and one formate or acetate through oxygen (Figure 1a, 1b). The Cd-O bond distances are 2.253 and 2.490 Å, and Cd-N distances of 2.264 and 2.303 Å. Each spiro-4-py ligand coordinates to four cadmium centers, forming (2, 4) connected one-dimensional chains running along b axis, which are further linked by pda, leading to a two-dimensional sheet on bc plane (Figure 1c). The resultant rhomboid grid has a vertex symbol of $\{3^6.4^6.5^3\}$ with ~10 Å openings. The pyridine moiety of the spiro-4-py ligand is not coplanar to the neighboring phenyl ring, resulting in a 12.10° torsion angle between them. The [π□□□π] stacking arrangements between pyridine rings and the phenyl rings from adjacent layers propagate these two-dimensional grids into the third dimension. The ring planes of the pyridine and phenyl involved in inter-layer [π□□□π] stacking are not parallel, and therefore interplanar distance cannot be determined. The closest C-C distance between the two rings is 3.64 Å (Figure 2). Interestingly, the stacking of these two-dimensional sheets does not block the openings, which results in one-dimensional channels running along c axis in the final structure (Figure 1d). The solvent accessible void is 26.2% of the crystal volume, calculated by PLATON.

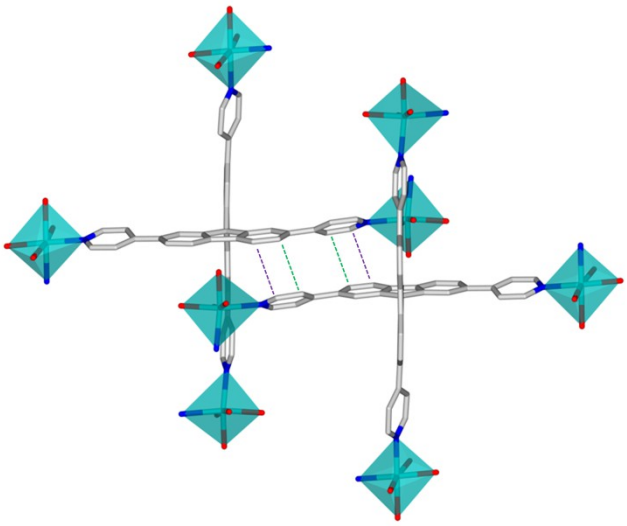

Figure 2. [π□□□π] arrangement from adjacent layers. Green (3.64 Å) and purple (3.69 Å) dashed lines represent the closest carbon-carbon distances.

The phase purity of both materials was confirmed by powder X-ray diffraction (PXRD, Figure S4). Thermogravimetric analysis (TGA) showed a weight loss (10-15 wt%) before 200 °C for both compounds, corresponding to solvent molecules inside the pore, followed by a plateau, indicating the materials are thermally stable up to 350 °C (Figure S1). In contrast to the poor moisture/water resistance commonly observed for coordination polymers built on late transition metals, compounds **1** and **2** exhibit excellent stability in aqueous solutions over a wide range of pH values. As shown in Figure S4, after being treated with aqueous solutions over a pH range of 2-10 (acidic and basic solutions were prepared from hydrochloric acid and sodium hydroxide aqueous solutions respectively with corresponding concentration to achieve different pH values) for 24 hours, both compounds maintained their crystallinity, confirmed by PXRD measurements. They also maintained intact structure after treatment with 80 °C water. The water stability of compounds **1** and **2** competes with that of most reported zirconium-based MOFs, which are known for their high water stability.[19,36-38]

Porosity characterization. Based on their crystal structures, the stacking of rhomboid grids yields one-dimensional open channels in compounds **1** and **2**. In order to confirm their permanent porosity, low temperature nitrogen adsorption measurements were performed on both compounds. As shown in Figure 3, at 77 K, compounds **1** and **2** take up 7.8 and 6.5 mmol/g nitrogen at P/P_0= 0.99, corresponding to pore volumes of 0.26 and 0.21 cm^3/g, respectively. The observed typical Type I isotherm profiles indicate the microporous nature of both compounds. The calculated BET surface areas are 687 m^2/g for compound **1** and 584 m^2/g for compound **2**. The difference in porosity should be attributed to their different terminal ligands. Replacing formate with acetate lowers the porosity due to the larger molecular size of the latter. Pore size distribution shows that the effective pore sizes of compounds **1** and **2** are 5.9 and 5.7 Å, respectively.

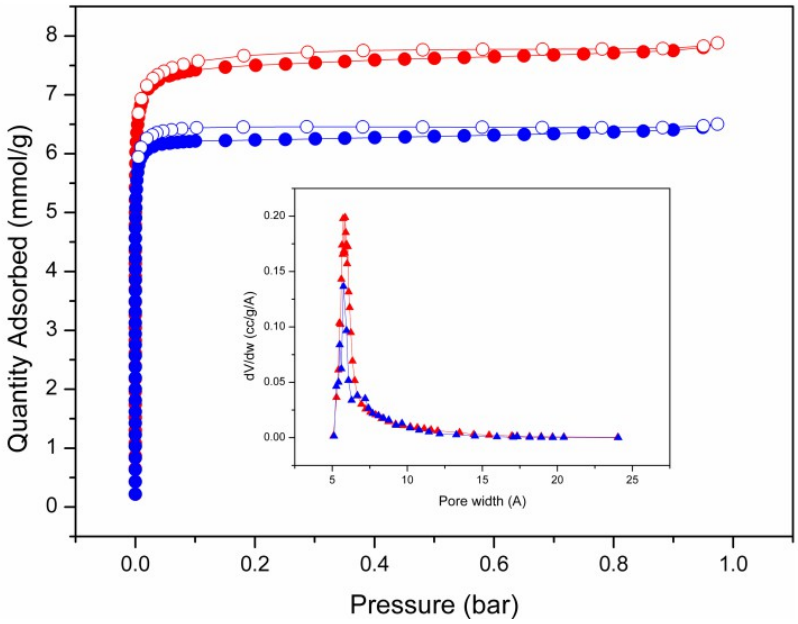

Figure 3. N_2 adsorption-desorption isotherms at 77 K for compounds **1** (red) and **2** (blue). The insert is their corresponding pore size distribution curve.

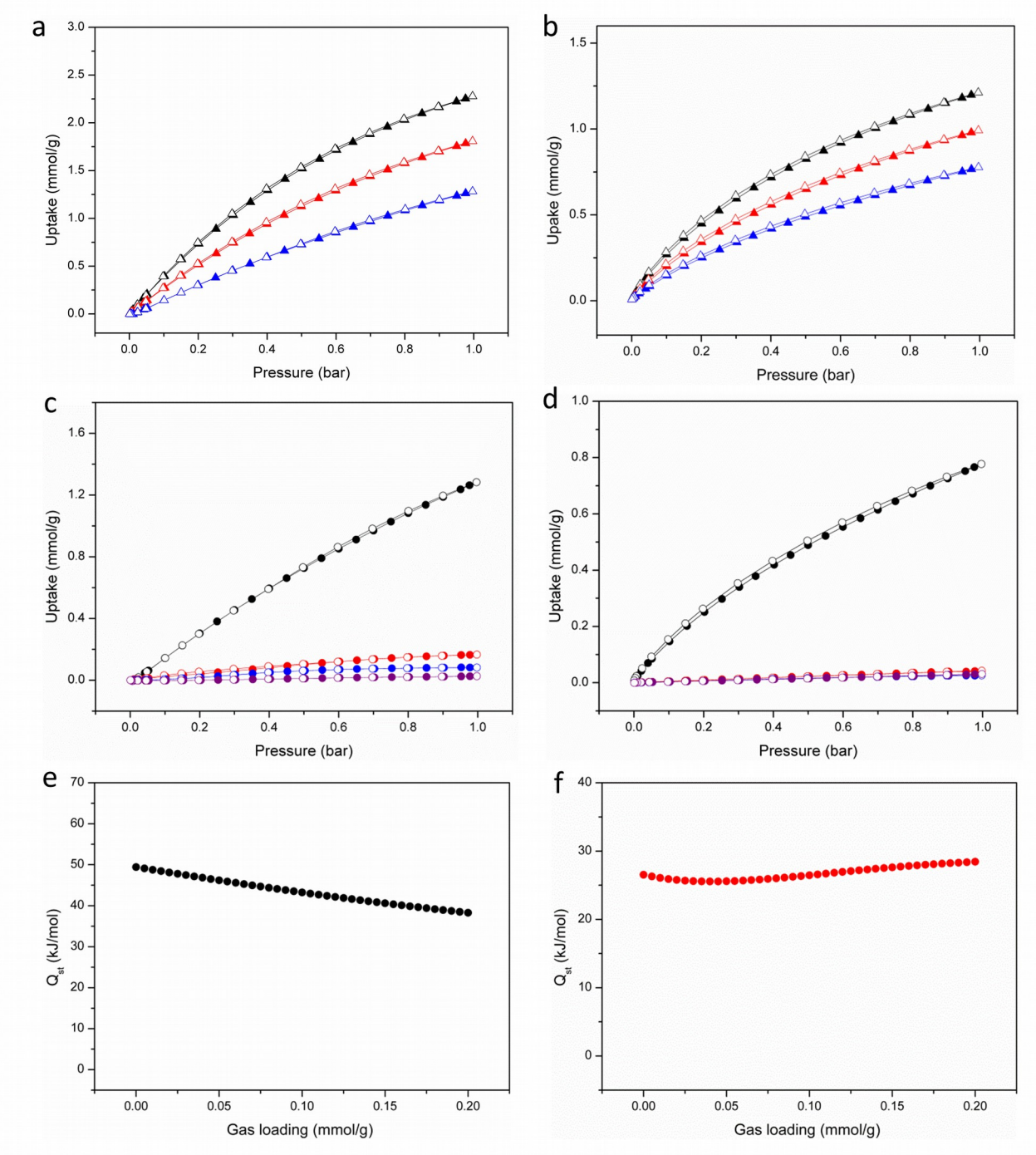

Figure 4. CO_2 adsorption-desorption isotherms at 278 K (black), 288 K (red), and 298 K (blue) for compounds **1** (a) and **2** (b). CO_2 adsorption-desorption isotherms of CO_2 (black), CO (red),

N_2 (blue), and O_2 (purple) at 298 K for compounds **1** (c) and **2** (d). Isosteric heats (Qst) of CO_2 adsorption for compounds **1** (e) and **2** (f).

Single component gas adsorption. High resistance towards moisture and the microporous nature of compounds **1** and **2** encouraged us to investigate these materials' performance in carbon dioxide capture. Carbon dioxide adsorption-desorption isotherms at three different temperatures (278 K, 288 K, 298 K) were collected on both compounds **1** and **2**. All isotherms are reversible, indicating their physisorption nature (Figure 4a, 4b). The carbon dioxide uptakes on compound **1** at 1 bar are 2.28, 1.81, and 1.28 mmol/g at 278 K, 288 K, and 298 K, respectively, while those for compound **2** are 1.21, 0.99, and 0.78 mmol/g. These values are consistent with the fact that compound **1** has a higher porosity than compound **2**. To evaluate the adsorption affinity, isosteric heats of adsorption (Q_{st}) were calculated with carbon dioxide adsorption isotherms at 278 K, 288 K, and 298 K. At zero coverage, the Q_{st} values for compounds **1** and **2** are 49 and 27 kJ/mol, respectively (Figure 4e, 4f). Higher affinity towards carbon dioxide on compound **1**, comparable to those of MOFs with open metal sites, is likely a result of the terminal formate acting as an electron-rich adsorption site.

Adsorption of other related light gases (nitrogen, oxygen, and carbon monoxide) was also investigated to evaluate if compounds **1** and **2** are able to discriminate these gases from carbon dioxide. The results show that both compounds take up negligible amounts of nitrogen, oxygen, or carbon monoxide at room temperature and 1 bar (Figure 4c, 4d). This suggests that compounds **1** and **2** favorably adsorb carbon dioxide over other light gases.

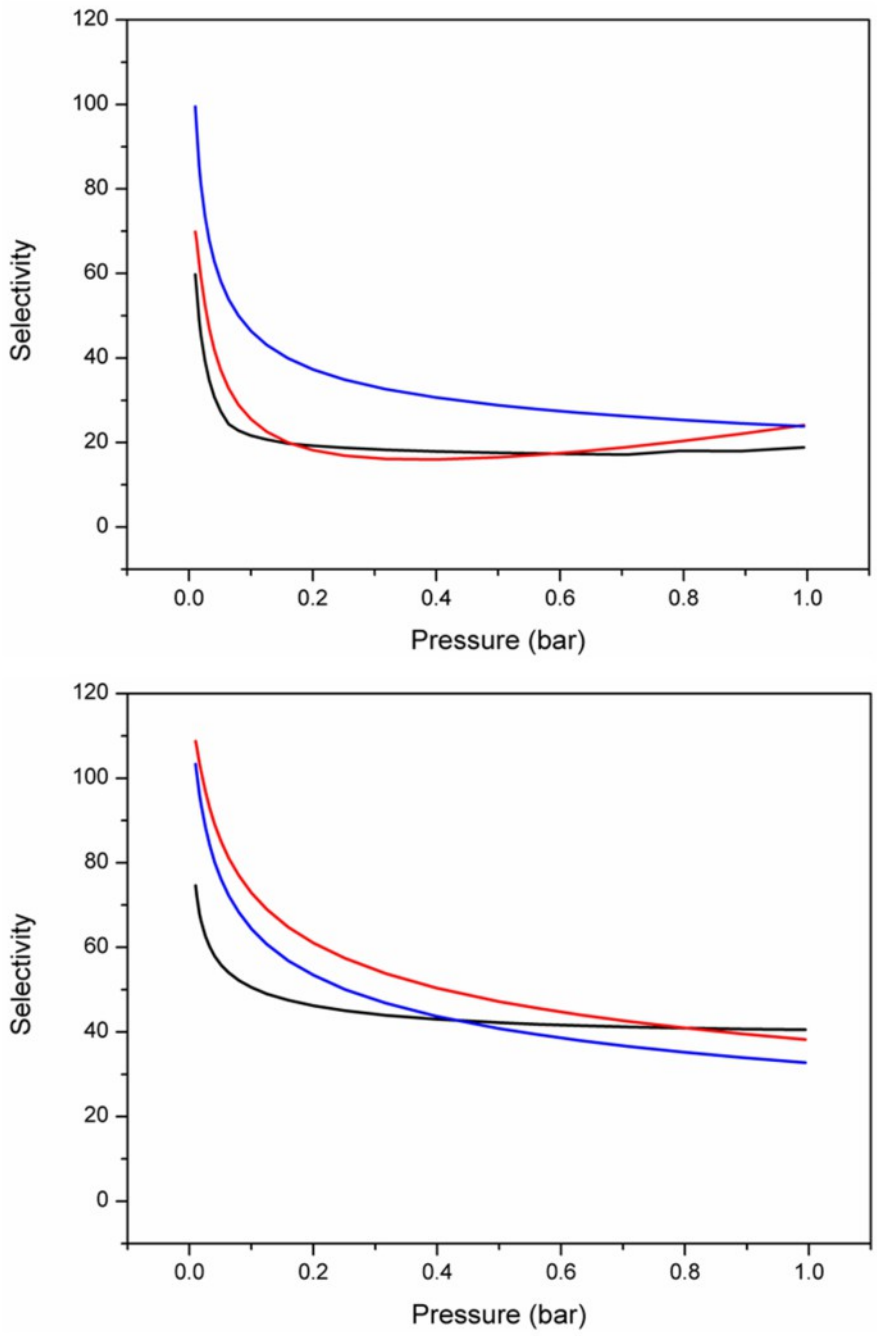

Figure 5. IAST adsorption selectivity for binary mixtures of CO_2/N_2= 20/80 (black), CO_2/CO= 50:50 (red) and CO_2/O_2= 50/50 (blue) for compounds **1** (top) and **2** (bottom).

IAST adsorption selectivity. The observed differences in the adsorption of carbon dioxide and other light gases (nitrogen, oxygen, and carbon monoxide) in compounds **1** and **2** suggest their preferred adsorption towards carbon dioxide. Ideal adsorbed solution theory (IAST)[30-33] was applied to quantitatively evaluate the carbon dioxide adsorption selectivities of compounds **1** and **2**. As a thermodynamic model for the prediction of multicomponent adsorption equilibrium from single component adsorption isotherms, IAST has been proven an effective technique for evaluating gas adsorption selectivity for various sorbent materials.[39-41] For binary gas mixtures of carbon dioxide:nitrogen = 20:80 (v:v), carbon dioxide:oxygen= 50:50 (v:v), and carbon dioxide:carbon monoxide = 50:50 (v:v), the calculated IAST adsorption selectivities of carbon dioxide over the other three gases are plotted out in Figure 5. For the aforementioned gas mixtures, compounds **1** and **2** show similar adsorption selectivity profiles. High adsorption selectivities (~ 60 - ~110) were observed at low pressure; these selectivities drop as the pressure increases and reach a plateau of ~ 40 and ~ 30 for compounds **1** and **2**, respectively. Similar to many reported microporous MOFs, the preferred adsorption toward carbon dioxide over other light gases observed here should be attributed to the higher quadruple moment of carbon dioxide molecules, leading to its stronger interaction with the pore surface of the sorbent.

CONCLUSIONS

In summary, two new isoreticular two-dimensional coordination polymers with permanent porosity were obtained, and their adsorption properties were investigated. Both compounds are built on a novel 4-connected spiro-4-py ligand and an auxiliary pda linker. Primary cadmium centers are connected by these two organic linkers to form two-dimensional rhomboid grids, which are propagated to the third dimension through interlayer [π□□□π] stacking. These

compounds show high thermal stability and exceptional water resistance. The microchannel in these compounds can selectively adsorb carbon dioxide over other light gases such as nitrogen and oxygen, as shown by single component isotherm measurements and IAST adsorption selectivity calculations. This study reveals that multipyridine ligands may play an important role in significantly enhancing water stability of late-transition metal based frameworks that are well-known for their instability towards water and moisture.

ASSOCIATED CONTENT

Supporting Information: The supporting information is available free of charge on the ACS Publications website at DOI: XXXXXXXXX. Crystal data, TGA, PXRD and isotherm fits.

AUTHOR INFORMATION

Corresponding Author: * jingli@rutgers.edu

ACKNOWLEDGMENTS

We acknowledge the support of the Department of Energy, Basic Energy Sciences, and Division of Materials Sciences and Engineering through Grant No. DE-FG02-08ER-46491. The Advanced Light Source is supported by the Director, Office of Science, Office of Basic Energy Sciences, of the U.S. Department of Energy under Contract No. DE-AC02-05CH11231. L.A. thanks the Natural Science Foundation of Jiangsu Provincial Department of Education (15KJA150003, 12KJD150002) and NSFC (21375044, 51602118).

REFERENCES

(1) Kitagawa, S.; Kitaura, R.; Noro, S.-i. Functional Porous Coordination Polymers. *Angew. Chem. Intl. Ed.* **2004**, *43*, 2334-2375.

(2) Zhou, H.-C.; Long, J. R.; Yaghi, O. M. Introduction to Metal–Organic Frameworks. *Chem. Rev.* **2012**, *112*, 673-674.

(3) Li, J.-R.; Sculley, J.; Zhou, H.-C. Metal–Organic Frameworks for Separations. *Chem. Rev.* **2012**, *112*, 869-932.

(4) Sumida, K.; Rogow, D. L.; Mason, J. A.; McDonald, T. M.; Bloch, E. D.; Herm, Z. R.; Bae, T.-H.; Long, J. R. Carbon Dioxide Capture in Metal–Organic Frameworks. *Chem. Rev.* **2012**, *112*, 724-781.

(5) Wu, H.; Gong, Q.; Olson, D. H.; Li, J. Commensurate Adsorption of Hydrocarbons and Alcohols in Microporous Metal Organic Frameworks. *Chem. Rev.* **2012**, *112*, 836-868.

(6) He, Y.; Zhou, W.; Qian, G.; Chen, B. Methane storage in metal-organic frameworks. *Chem. Soc. Rev.* **2014**, *43*, 5657-5678.

(7) Wang, H.; Yao, K.; Zhang, Z.; Jagiello, J.; Gong, Q.; Han, Y.; Li, J. The first example of commensurate adsorption of atomic gas in a MOF and effective separation of xenon from other noble gases. *Chem. Sci.* **2014**, *5*, 620-624.

(8) Tzoulaki, D.; Heinke, L.; Lim, H.; Li, J.; Olson, D.; Caro, J.; Krishna, R.; Chmelik, C.; Kaerger, J. Assessing Surface Permeabilities from Transient Guest Profiles in Nanoporous Host Materials. *Angew. Chem. Intl. Ed.* **2009**, *48*, 3525-3528.

(9) Nijem, N.; Thissen, P.; Yao, Y.; Longo, R. C.; Roodenko, K.; Wu, H.; Zhao, Y.; Cho, K.; Li, J.; Langreth, D. C.; Chabal, Y. J. Understanding the Preferential Adsorption of CO(2) over N(2) in a Flexible Metal-Organic Framework. *J J. Am. Chem. Soc.* **2011**, *133*, 12849-12857.

(10) Liu, H.; Zhao, Y. G.; Zhang, Z. J.; Nijem, N.; Chabal, Y. J.; Zeng, H. P.; Li, J. The Effect of Methyl Functionalization on Microporous Metal-Organic Frameworks' Capacity and Binding Energy for Carbon Dioxide Adsorption. *Adv. Funct. Mater.* **2011**, *21*, 4754-4762.

(11) Liao, P.-Q.; Chen, X.-W.; Liu, S.-Y.; Li, X.-Y.; Xu, Y.-T.; Tang, M.; Rui, Z.; Ji, H.; Zhang, J.-P.; Chen, X.-M. Putting an ultrahigh concentration of amine groups into a metal-organic framework for CO2 capture at low pressures. *Chem. Sci.* **2016**, *7*, 6528-6533.

(12) Chen, B.; Xiang, S.; Qian, G. Metal−Organic Frameworks with Functional Pores for Recognition of Small Molecules. *Acc. Chem. Res.* **2010**, *43*, 1115-1124.

(13) Wang, H.; Peng, J.; Li, J. Ligand Functionalization in Metal–Organic Frameworks for Enhanced Carbon Dioxide Adsorption. *Chem. Rec.* **2016**, *16*, 1298-1310.

(14) Furukawa, H.; Go, Y. B.; Ko, N.; Park, Y. K.; Uribe-Romo, F. J.; Kim, J.; O'Keeffe, M.; Yaghi, O. M. Isoreticular Expansion of Metal–Organic Frameworks with Triangular and Square Building Units and the Lowest Calculated Density for Porous Crystals. *Inorg. Chem.* **2011**, *50*, 9147-9152.

(15) Guillerm, V.; Ragon, F.; Dan-Hardi, M.; Devic, T.; Vishnuvarthan, M.; Campo, B.; Vimont, A.; Clet, G.; Yang, Q.; Maurin, G.; Férey, G.; Vittadini, A.; Gross, S.; Serre, C. A Series of Isoreticular, Highly Stable, Porous Zirconium Oxide Based Metal–Organic Frameworks. *Angew. Chem. Intl. Ed.* **2012**, *51*, 9267-9271.

(16) Deng, H.; Grunder, S.; Cordova, K. E.; Valente, C.; Furukawa, H.; Hmadeh, M.; Gándara, F.; Whalley, A. C.; Liu, Z.; Asahina, S.; Kazumori, H.; O'Keeffe, M.; Terasaki, O.;

Stoddart, J. F.; Yaghi, O. M. Large-Pore Apertures in a Series of Metal-Organic Frameworks. *Science* **2012**, *336*, 1018-1023.

(17) Fu, Y.; Sun, D.; Chen, Y.; Huang, R.; Ding, Z.; Fu, X.; Li, Z. An Amine-Functionalized Titanium Metal–Organic Framework Photocatalyst with Visible-Light-Induced Activity for CO2 Reduction. *Angew. Chem. Intl. Ed.* **2012**, *51*, 3364-3367.

(18) Li, B.; Leng, K.; Zhang, Y.; Dynes, J. J.; Wang, J.; Hu, Y.; Ma, D.; Shi, Z.; Zhu, L.; Zhang, D.; Sun, Y.; Chrzanowski, M.; Ma, S. Metal–Organic Framework Based upon the Synergy of a Brønsted Acid Framework and Lewis Acid Centers as a Highly Efficient Heterogeneous Catalyst for Fixed-Bed Reactions. *J. Am. Chem. Soc.* **2015**, *137*, 4243-4248.

(19) Bai, Y.; Dou, Y.; Xie, L.-H.; Rutledge, W.; Li, J.-R.; Zhou, H.-C. Zr-based metal-organic frameworks: design, synthesis, structure, and applications. *Chem. Soc. Rev.* **2016**, *45*, 2327-2367.

(20) He, Y.; Li, B.; O'Keeffe, M.; Chen, B. Multifunctional metal-organic frameworks constructed from meta-benzenedicarboxylate units. *Chem. Soc. Rev.* **2014**, *43*, 5618-5656.

(21) Xiang, S.; He, Y.; Zhang, Z.; Wu, H.; Zhou, W.; Krishna, R.; Chen, B. Microporous metal-organic framework with potential for carbon dioxide capture at ambient conditions. *Nat. Commun.* **2012**, *3*, 954-962.

(22) Nugent, P.; Belmabkhout, Y.; Burd, S. D.; Cairns, A. J.; Luebke, R.; Forrest, K.; Pham, T.; Ma, S.; Space, B.; Wojtas, L.; Eddaoudi, M.; Zaworotko, M. J. Porous materials with optimal adsorption thermodynamics and kinetics for CO2 separation. *Nature* **2013**, *495*, 80-84.

(23) McDonald, T. M.; Mason, J. A.; Kong, X.; Bloch, E. D.; Gygi, D.; Dani, A.; Crocella, V.; Giordanino, F.; Odoh, S. O.; Drisdell, W. S.; Vlaisavljevich, B.; Dzubak, A. L.; Poloni, R.; Schnell, S. K.; Planas, N.; Lee, K.; Pascal, T.; Wan, L. F.; Prendergast, D.; Neaton, J. B.; Smit, B.; Kortright, J. B.; Gagliardi, L.; Bordiga, S.; Reimer, J. A.; Long, J. R. Cooperative insertion of CO2 in diamine-appended metal-organic frameworks. *Nature* **2015**, *519*, 303-308.

(24) Zhang, Z.; Zhao, Y.; Gong, Q.; Li, Z.; Li, J. MOFs for CO2 capture and separation from flue gas mixtures: the effect of multifunctional sites on their adsorption capacity and selectivity. *Chem. Commun.* **2013**, *49*, 653-661.

(25) Li, J.-R.; Ma, Y.; McCarthy, M. C.; Sculley, J.; Yu, J.; Jeong, H.-K.; Balbuena, P. B.; Zhou, H.-C. Carbon dioxide capture-related gas adsorption and separation in metal-organic frameworks. *Coord. Chem. Rev.* **2011**, *255*, 1791-1823.

(26) Zhang, Z.; Yao, Z.-Z.; Xiang, S.; Chen, B. Perspective of microporous metal-organic frameworks for CO2 capture and separation. *Energy Environ. Sci.* **2014**, *7*, 2868-2899.

(27) Nagarkar, S. S.; Chaudhari, A. K.; Ghosh, S. K. Selective CO2 Adsorption in a Robust and Water-Stable Porous Coordination Polymer with New Network Topology. *Inorg. Chem.* **2012**, *51*, 572-576.

(28) Jagiełło, J.; Bandosz, T. J.; Schwarz, J. A. Characterization of Microporous Carbons Using Adsorption at Near Ambient Temperatures. *Langmuir* **1996**, *12*, 2837-2842.

(29) Czepirski, L.; JagieŁŁo, J. Virial-type thermal equation of gas—solid adsorption. *Chem. Eng. Sci.* **1989**, *44*, 797-801.

(30) Bae, Y.-S.; Farha, O. K.; Spokoyny, A. M.; Mirkin, C. A.; Hupp, J. T.; Snurr, R. Q. Carborane-based metal-organic frameworks as highly selective sorbents for CO2 over methane.*Chem. Commun.* **2008**, 4135-4137.

(31) Bae, Y.-S.; Mulfort, K. L.; Frost, H.; Ryan, P.; Punnathanam, S.; Broadbelt, L. J.; Hupp, J. T.; Snurr, R. Q. Separation of CO2 from CH4 Using Mixed-Ligand Metal−Organic Frameworks. *Langmuir* **2008**, *24*, 8592-8598.

(32) Heuchel, M.; Snurr, R. Q.; Buss, E. Adsorption of CH4−CF4 Mixtures in Silicalite: Simulation, Experiment, and Theory. *Langmuir* **1997**, *13*, 6795-6804.

(33) Myers, A. L.; Prausnitz, J. M. Thermodynamics of mixed-gas adsorption. *AIChE J.* **1965**, *11*, 121-127.

(34) Davies, R. P.; Less, R.; Lickiss, P. D.; Robertson, K.; White, A. J. P. Structural Diversity in Metal−Organic Frameworks Built from Rigid Tetrahedral [Si(p-C6H4CO2)4]4− Struts. *Cryst. Growth Des.* **2010**, *10*, 4571-4581.

(35) Hao, X.-R.; Wang, X.-L.; Su, Z.-M.; Shao, K.-Z.; Zhao, Y.-H.; Lan, Y.-Q.; Fu, Y.-M. Two unprecedented porous anionic frameworks: organoammonium templating effects and structural diversification. *Dalton Trans.* **2009**, 8562-8566.

(36) Feng, D.; Gu, Z.-Y.; Li, J.-R.; Jiang, H.-L.; Wei, Z.; Zhou, H.-C. Zirconium-Metalloporphyrin PCN-222: Mesoporous Metal–Organic Frameworks with Ultrahigh Stability as Biomimetic Catalysts. *Angew. Chem. Intl. Ed.* **2012**, *51*, 10307-10310.

(37) Deria, P.; Gómez-Gualdrón, D. A.; Bury, W.; Schaef, H. T.; Wang, T. C.; Thallapally, P. K.; Sarjeant, A. A.; Snurr, R. Q.; Hupp, J. T.; Farha, O. K. Ultraporous, Water Stable, and Breathing Zirconium-Based Metal–Organic Frameworks with ftw Topology. *J. Am. Chem. Soc.* **2015**, *137*, 13183-13190.

(38) Banerjee, D.; Xu, W.; Nie, Z.; Johnson, L. E. V.; Coghlan, C.; Sushko, M. L.; Kim, D.; Schweiger, M. J.; Kruger, A. A.; Doonan, C. J.; Thallapally, P. K. Zirconium-Based Metal–Organic Framework for Removal of Perrhenate from Water. *Inorg. Chem.* **2016**, 55, 8241-8243

(39) Zhang, Z.; Liu, J.; Li, Z.; Li, J. Experimental and theoretical investigations on the MMOF selectivity for CO2vs. N2 in flue gas mixtures. *Dalton Trans.* **2012**, *41*, 4232-4238.

(40) Mason, J. A.; Sumida, K.; Herm, Z. R.; Krishna, R.; Long, J. R. Evaluating metal-organic frameworks for post-combustion carbon dioxide capture via temperature swing adsorption. *Energy Environ. Sci.* **2011**, *4*, 3030-3040.

(41) Chen, J.; Loo, L. S.; Wang, K. An Ideal Absorbed Solution Theory (IAST) Study of Adsorption Equilibria of Binary Mixtures of Methane and Ethane on a Templated Carbon. *J. Chem. Eng. Data* **2011**, *56*, 1209-1212.

For Table of Contents Only

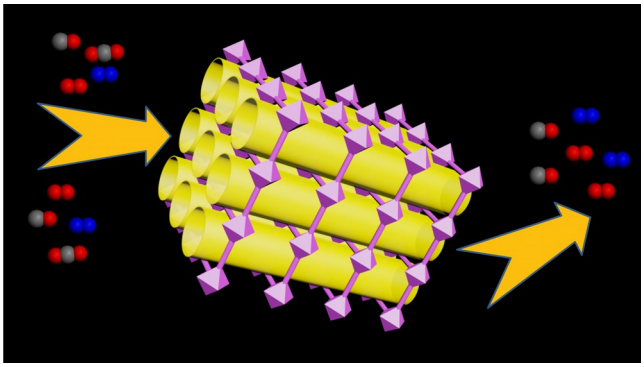

Two new and robust porous coordination polymers made of dicarboxylate and tetrapyridine based organic ligands have been synthesized and structurally characterized. Both compounds exhibit excellent stability in aqueous solutions of a wide pH range and highly selective adsorption towards carbon dioxide over other small gases.